Fuchsman, W. H., & Appleby, C. A. (1979) *Biochemistry 18*, 1309–1321.
Ho, C., & Russu, I. M. (1981) *Methods Enzymol. 76*, 275–312.
Huang, T.-H. (1979) Ph.D. Thesis, Brandeis University, Waltham, MA.
Ikeda-Saito, M., Iizuka, T., Yamamoto, H., Kayne, F. J., & Yonetani, T. (1977) *J. Biol. Chem. 252*, 4882–4887.
Johnson, M. E., Fung, L. W.-M., & Ho, C. (1977) *J. Am. Chem. Soc. 99*, 1245–1250.
Kalk, A., & Berendsen, H. J. C. (1976) *J. Magn. Reson. 24*, 343–366.
Keller, R. M., & Wüthrich, K. (1981) *Biol. Magn. Reson. 3*, 1–52.
Kilmartin, J. V., Fogg, J., Luzzana, M., & Rossi-Bernardi, L. (1973) *J. Biol. Chem. 248*, 7039–7043.
Kilmartin, J. V., Hewitt, J. A., & Wootton, J. F. (1975) *J. Mol. Biol. 93*, 203–218.
Lindstrom, T. R., & Ho, C. (1972) *Proc. Natl. Acad. Sci. U.S.A. 69*, 1707–1710.
Lindstrom, T. R., & Ho, C. (1973) *Biochemistry 12*, 134–139.
Lindstrom, T. R., Nor'en, I. B. E., Charache, S., Lehmann, H., & Ho, C. (1972) *Biochemistry 11*, 1677–1681.
Mabbutt, B. C., & Wright, P. E. (1983) *Biochim. Biophys. Acta 744*, 281–290.
McDonald, C. C., & Phillips, W. D. (1969) *J. Am. Chem. Soc. 91*, 1513–1521.
Mims, M. P., Olson, J. S., Russu, I. M., Miura, S., Cedel, T. E., & Ho, C. (1983) *J. Biol. Chem. 258*, 6125–6134.
Moffat, K., Deatherage, J. F., & Seybert, D. W. (1979) *Science (Washington, D.C.) 206*, 1035–1042.
Noggle, J. H., & Schirmer, R. E. (1971) *The Nuclear Overhauser Effect: Chemical Applications*, Academic Press, New York.
Olson, J. S., Mims, M. P., & Reisberg, P. I. (1982) in *Hemoglobin and Oxygen Binding* (Ho, C., Eaton, W. A., Collman, J. P., Gibson, Q. H., Leigh, J. S., Jr., Margoliash, E., Moffat, K., & Scheidt, W. R., Eds.) pp 393–398, Elsevier/North-Holland, New York.
Perutz, M. F. (1970) *Nature (London) 228*, 726–739.
Poulsen, F. M., Hoch, J. C., & Dobson, C. M. (1980) *Biochemistry 19*, 2597–2607.
Russu, I. M., Ho, N. T., & Ho, C. (1982) *Biochemistry 21*, 5031–5043.
Shaanan, B. (1983) *J. Mol. Biol. 171*, 31–59.
Solomon, I. (1955) *Phys. Rev. 99*, 559–565.
Stoesz, J. D., Malinowski, D. P., & Redfield, A. G. (1979) *Biochemistry 18*, 4669–4675.
Valdes, R., Jr., & Ackers, G. K. (1977) *J. Biol. Chem. 252*, 74–81.
Wagner, G., Kumar, A., & Wüthrich, K. (1981) *Eur. J. Biochem. 114*, 375–384.
Wider, G., Lee, K. H., & Wüthrich, K. (1982) *J. Mol. Biol. 155*, 367–388.

NMR Relaxation of Protein and Water Protons in Diamagnetic Hemoglobin Solutions†

Maurice Eisenstadt
Department of Medicine, Albert Einstein College of Medicine, Bronx, New York 10461
Received October 18, 1984

ABSTRACT: We have measured T_1 and T_2 of protein and water protons in hemoglobin solutions using broad-line pulse techniques; selective excitation and detection methods enabled the intrinsic protein and water relaxation rates, as well as the spin-transfer rate between them, to be obtained at 5, 10, and 20 MHz. Water and protein T_1 data were also obtained at 100 and 200 MHz for hemoglobin in H_2O/D_2O mixtures by using commercial Fourier-transform instruments. The T_1 data conform to a simple model of two well-mixed spin systems with single intrinsic relaxation times and an average spin-transfer rate, with each phase recovering from a radio-frequency excitation with a biexponential time dependence. At low frequencies, protein T_1 and T_2 agree reasonably with a model of dipolar relaxation of an array of fixed protons tumbling in solution, explicitly calculating methyl and methylene relaxation and using a continuum approximation for the others. Differing values in H_2O and D_2O are mainly ascribed to solvent viscosity. For water-proton relaxation, T_1, T_2, and spin transfer were measured for H_2O and HDO, which enabled a separation of inter- and intramolecular contributions to relaxation. Despite such detail, few firm conclusions could be reached about hydration water. But it seems clear that few long-lived hydration sites are needed to explain T_1 and T_2, and the spin-transfer value mandates fewer than five sites with a lifetime longer than 10^{-8} s.

The hydration water of biological macromolecules has been studied with a variety of techniques, but its characterization remains vague and controversial. The time scales of the different methods vary widely, making comparisons difficult. Such questions have been thoroughly reviewed (Kuntz & Kauzmann, 1974). Packer (1977) has reviewed the role of water in more general heterogeneous systems, with emphasis on nuclear magnetic resonance (NMR)[1] work. NMR relaxation measurements provide a unique probe of the microscopic nature of hydration water, because the interactions responsible for relaxation are very short range. Studies of water relaxation

† This work was supported by USPHS Grant HL 17571.

[1] Abbreviations: NMR, nuclear magnetic resonance; FT, Fourier transform; MHz, megahertz; BPTI, basic pancreatic trypsin inhibitor; Hb, hemoglobin; M_r, molecular weight; NOE, nuclear Overhauser effect; CPMG, Carr–Purcell–Meiboom–Gill; FID, free induction decay; A/D, analog to digital; S/N, signal to noise; ZPC, zero-point crossing; WS, water suppression; rf, radio frequency; INV, inversion; TMV, tobacco mosaic virus; FET, field effect transistor.

0006-2960/85/0424-3407$01.50/0

over a wide frequency range[2] have been of particular value (Hallenga & Koenig, 1976; Grosch & Noack, 1976), since they effectively explore a broad time scale. There is no question that the magnetic dipolar relaxation of water protons reflects the overall tumbling of the macromolecule, as does quadrupolar relaxation of deuterons in protein–D_2O solution (Hallenga & Koenig, 1976). Yet severe inconsistencies arise when interpreting relaxation data in terms of simple hydration models.

Early water proton T_1 experiments in protein solutions focused attention almost exclusively on the water spin system, assuming the solute only affected the dynamics of the water intramolecular proton–proton dipolar interaction. By 1978, it was clear that the protein–proton spins played an important role, even if only the water protons were measured (Eisenstadt & Fabry, 1978; Koenig et al., 1978). T_2 in such systems has been much less studied (Grosch & Noack, 1976; Thompson et al., 1975; Zipp et al., 1976).

Protein–proton NMR spectra were obtained even earlier than the above experiments (Saunders et al., 1957), but only showed a few broad peaks, at the frequencies available at that time (60 MHz and lower). Subsequent work has pushed to ever higher frequencies, and at present, two-dimensional Fourier-transform (FT) spectra at 500 MHz can assign a line to virtually every proton of a light protein such as BPTI (M_r 6500) (Wagner & Wuthrich, 1982). Relaxation times, spin transfer, and the role of the water protons have also been studied, but the vastly different frequency domain from the above water studies makes the connection with the latter tenuous; for typical protein solutions, water T_1 undergoes its most dramatic changes in the range 0.5–50 MHz (Hallenga & Koenig, 1976).

We have been measuring T_1 and T_2 of water and protein protons, mainly at 5, 10, and 20 MHz, but with some FT relaxation spectra at 100 and 200 MHz. All of the work reported here is with hemoglobin (Hb; M_r 68 000), although the generalization to other globular proteins should be legitimate. Compared to the spectrum of BPTI, the spectrum of Hb is largely a mass of unresolved lines, due both to the greater number of protons and to the slower tumbling of a heavier molecule in solution. In fact, from our T_2 measurements shown below, the line width of a single backbone proton at 20 MHz would be broader than the chemical shift range of the entire spectrum.

Despite this, there are numerous interesting NMR parameters to measure, particularly when the protein and water spin systems are viewed in a unified way. T_1 and T_2 are obtained for the protein and water protons separately by using selective detection methods described below. The amplitudes of these separate components in both T_1 and T_2 measurements also have considerable meaning. In particular, when only one of the spin systems is inverted in a T_1 experiment, the amplitude of the other yields the spin-transfer rate between them, much like the nuclear Overhauser effect (NOE). Deuteration of the solvent water eliminates the contribution of solvent protons to protein proton relaxation; at the same time, T_1 of the remaining few HDO protons is missing the intramolecular contribution of the other water proton. The frequency dependence of the protein proton relaxation is especially revealing, even over our truncated frequency range. Finally, the physiochemical parameters of concentration and temperature can be varied.

For hemoglobin, an important further resource is to measure NMR relaxation in red cell suspensions (Eisenstadt & Fabry, 1978). For purposes here, the red cell is simply a sack of concentrated Hb solution, 5.4 mM at normal osmolarity. Through the use of millimolar amounts of Mn^{2+} in the extracellular phase, water relaxation may be drastically shortened, without changing the intrinsic protein relaxation (since the membrane is impermeable to Hb and Mn but highly permeable to water, on our time scale of seconds to milliseconds). The tumbling time of Hb can be changed by changing its intracellular concentration through osmotic manipulation, while its overall concentration (on which the water relaxation mainly depends) is left unchanged by keeping the number of cells constant. In effect, we have a microscopic semipermeable membrane to aid in separating the many relaxation effects. Also, the cell water lifetime, a number we know very well (Fabry & Eisenstadt, 1978), acts as a natural clock in comparing spin transfer with atomic transfer. This work verified, in a novel way, the spin exchange between protein and water systems.

With so many different protein protons in so many different environments, one might expect a time-domain T_1 or T_2 measurement to yield a broad distribution of values, of as little use as the frequency-domain spectrum. Indeed the measured protein T_2 is a distribution; nonetheless, it is very useful, as discussed later. But early on in our Hb red cell work (Fabry & Eisenstadt, 1978) we observed that, after a brief induction period, all protein spins relaxed as a unit, with the same T_1. This was explained very succinctly by Kalk & Berendsen (1976), although earlier work presaged several aspects (Kimmich & Noack, 1970). They assumed that various spin groups i (e.g., methyl protons) have a local relaxation rate R_{1i} for the transfer of spin energy to the "lattice" and a transfer rate R_{tij} for the exchange of spin energy with other groups j. The magnetic dipolar interaction between spins is responsible for both rates. R_{tij} is closely related to a third rate, the local spin–spin relaxation rate R_{2i}. For diamagnetic proteins at frequencies above a few megahertz, R_{tij} and R_{2i} are much bigger than R_{1i}. As a consequence, when the protein spin system is inverted, within a time of the order of $1/R_t$, they equilibrate among themselves and relax back to their normal orientation at a single average R_1. This is a very thermodynamic (albeit nonequilibrium) viewpoint; the nuclei quickly come to the same spin temperature and then together relax more slowly to the lattice temperature.

The initial process is sometimes known as spin diffusion, by analogy with atomic diffusion, and ensures that the protein spin system is "well mixed", i.e., that all protein spins are equivalent in a T_1 measurement. The same considerations apply to the solvent water protons, but they mix via atomic diffusion alone. They also exist in a variety of magnetic environments, mainly in the bulk surrounded by other water spins, but in concentrated Hb solutions many are adjacent to protein spins, and have a much faster local relaxation rate. Here too, we assume that the water molecules exchange between the hydration region and the bulk more rapidly than any local relaxation time, and all of the water spins relax with a single average relaxation time. At our lowest frequency of 5 MHz, this would demand that the lifetime in the hydration region be less than about a millisecond; we see no evidence in our work (discussed later) or that of others that any significant amount of water would persist this long.

Finally, one must consider spin transfer between the solvent and the protein spin systems. This is distinct from (although

[2] Throughout this paper we describe the magnetic field strength in terms of the proton Larmor frequency at that field. For our experiments the relationship is unambiguous, but for multinuclear work, or systems with electron paramagnetic relaxation agents, more care would be called for.

related to) the local R_{1h} of hydration water; the latter gives spin energy to the lattice, but the former conserves the total spin energy. If the water spins alone were measured, the two processes would be indistinguishable. Just as for the interactions among protein spins, the water–protein spin-transfer rate is closely related to the contribution of the protein protons to the water T_2.

The detailed mechanisms for relaxation and spin transfer depend on the microscopic model of hydration water. We will consider this later. But a phenomenological model of two-phase exchange has been used by ourselves and others (Eisenstadt & Fabry, 1978; Koenig et al., 1978) to explain the basic features of relaxation in these systems, using only the intrinsic relaxation times, the average exchange or spin-transfer rates, and the spin populations in each phase. Many valuable conclusions can be drawn even at this level. Furthermore, a minimum requirement before attempting any molecular interpretation is to derive these rates from the data.

Exchange Formulation of Relaxation Rates

We will briefly outline this treatment. The solutions to the differential equations can be found in any applied mathematics text, and in a previous publication we discussed NMR and exchange in great detail (Eisenstadt, 1980a). The time evolution of the nuclear magnetization of the protein and water phases (spin systems), M_P and M_A, after being displaced from their equilibrium direction at time zero, is given by the coupled first-order differential equations

$$d\Delta M_P(t)/dt = -(R_{1,2p} + k_s)\Delta M_P(t) + k_t\Delta M_A(t) \quad (1a)$$

$$d\Delta M_A(t)/dt = -(R_{1,2a} + k_t)\Delta M_A(t) + k_s\Delta M_P(t) \quad (1b)$$

These equations apply to T_1 or T_2 by using the subscript 1 or 2. The magnetizations are expressed as deviations from their equilibrium value; i.e., for a T_1 experiment, $\Delta M_P(t) = M_P(t) - M_P^0$, where M_P^0 is the equilibrium magnetization of the protein phase, and for a T_2 experiment, $\Delta M_P(t) = M_P(t)$. The rate k_s is the first-order rate of transfer of magnetization from phase P to A, and k_t is the reverse. These equations are so general that k_s and k_t can be actual atomic hydrogen exchange, or exchange of spin only; however, the latter process only is relevent in T_1 experiments. By doing both experiments, it may be possible to distinguish the two types of exchange (Eisenstadt, 1980b). As emphasized above, the intrinsic rates $R_{1,2A}$ depend very much on the protein concentration, but they pertain only to the direct transfer of energy to the lattice (R_{1a}) or independent loss of coherence (R_{2a}).

The solutions to the rate equations for T_1 are the sums of two exponentials:

$$\Delta M_P(t) = M_{P+}\exp(-\phi_{1+}t) + M_{P-}\exp(-\phi_{1-}t) \quad (2a)$$

$$\Delta M_A(t) = M_{A+}\exp(-\phi_{1+}t) + M_{A-}\exp(-\phi_{1-}t) \quad (2b)$$

$$2\phi_{1\pm} = (R_{1p} + k_s + R_{1a} + k_t) \pm [(R_{1p} + k_s - R_{1a} - k_t)^2 + 4k_sk_t]^{1/2} \quad (3)$$

$$(\phi_{1+} - \phi_{1-})M_{P+} = (R_{1p} + k_s - \phi_{1-})\Delta M_{P0} - k_t\Delta M_{A0} \quad (4a)$$

$$(\phi_{1+} - \phi_{1-})M_{P-} = (\phi_{1+} - R_{1p} - k_s)\Delta M_{P0} + k_t\Delta M_{A0} \quad (4b)$$

$$(\phi_{1+} - \phi_{1-})M_{A+} = (R_{1a} + k_t - \phi_{1-})\Delta M_{A0} - k_s\Delta M_{P0} \quad (4c)$$

$$(\phi_{1+} - \phi_{1-})M_{A-} = (\phi_{1+} - R_{1a} - k_t)\Delta M_{A0} + k_s\Delta M_{P0} \quad (4d)$$

$$M_{P+} + M_{P-} = \Delta M_{P0} \equiv M_{P0} - M_P^0$$
$$M_{A+} + M_{A-} = \Delta M_{A0} \equiv M_{A0} - M_A^0 \quad (4e)$$

M_{P0} and M_{A0} are the initial values after some preparative pulse sequence and ΔM_{P0} and ΔM_{A0} their deviation from equilibrium, as above. For T_2 experiments, substitute 2 for 1. The fast and slow decay rates are denoted by subscripts (+) and (−), respectively. Since all evidence shows (see Data Analysis) that every proton in the sample contributes to the NMR signal, we take the equilibrium magnetizations as strictly proportional to the proton populations of each phase, N_P and N_A; these are known from stoichiometry and measured protein optical spectra (see below).

Rigorous application of these equations requires that all spins in each phase be equivalent, i.e., well mixed. Furthermore, since the experiments are all at chemical equilibrium, the populations of each phase are constant. Then the overall transfer rates are related through detailed balance, $N_Pk_s = N_Ak_t$, and there remain three unknown rates to be determined in a given T_1 or T_2 experiment. The question of equivalence merits discussion. In the solvent phase, it means that water protons exchange rapidly between regions of different local relaxation times, so a single average $R_{1,2a}$ is valid. Likewise, they exchange rapidly with regions of different local spin or atomic transfer with protein protons, so k_t is also a valid average. Water diffusion is so rapid that good solvent spin mixing seems assured; in any case, ample experimental evidence is presented below.

Good protein spin mixing is less obvious, since spin diffusion is much slower than atomic diffusion (Abragam, 1961). For T_1 experiments, this question has been examined in great detail in another publication (Eisenstadt, 1981). There, protein T_1 was measured in metHb, where the paramagnetic heme sites provided four regions of strong local relaxation. In D_2O solvent at 20 MHz, within about 20 ms after excitation, all protein spins relaxed back to equilibrium as a unit. For the T_1 measurements of the present paper on diamagnetic (carbon monoxy)hemoglobin, there are no such powerful and isolated relaxation centers, and with few exceptions, protein spin mixing is complete in a few milliseconds. Strong evidence for this, at 20 MHz in D_2O, is shown under Data Analysis. As discussed later, methyl protons act as relaxation sinks; since they are numerous, spread throughout the protein, and much weaker than the hemes, observable relaxation differences among protein protons should damp out quickly, even though the spin-diffusion constant should be independent of the strength of the sink.

As the frequency is lowered, this assumption must inevitably break down, since for the magnetic dipolar interaction, the spin-transfer rate is proportional to protein T_2, and protein T_1 approaches T_2 at low frequencies (see eq 7 and 8). For our most dilute samples at 5 MHz, there is some indication of poor mixing. At *any* frequency, protein T_2 measurements yield a distribution of values, so eq 1 will not strictly apply. But all protein T_2 components are some 2 orders of magnitude faster than water T_2, so useful information on exchange can be obtained from the single and dominant slow component of T_2, as discussed later.

Experimental Procedures

Hemoglobin samples were freshly prepared from the author's blood by using procedures described elsewhere (Eisenstadt, 1981). The protein was immediately converted to the carboxy form by bubbling CO through the suspended cells for 2 h, to ensure greater stability against conversion to the paramagnetic metHb. The most sensitive NMR monitor of metHb is water T_2; the reproducibility of the latter was checked after any long series of runs. All data with Hb in H_2O were taken within 3 days of preparation, and in D_2O, 5 days. When not being measured, samples were stored at 4 °C under a CO atmosphere.

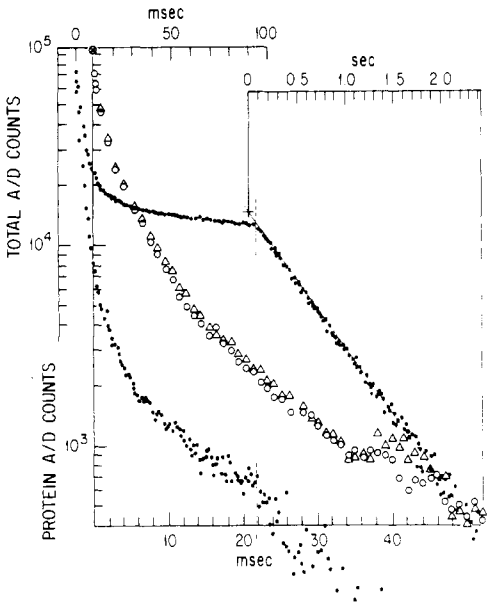

FIGURE 1: Spin-echo data for 3.6 mM Hb in largely D_2O at 25 °C, 20 MHz. Upper points and upper time scales: conventional CPMG experiment. After echo 100, only every 20th echo is recorded, hence the compressed time scale. Lower points and upper time scales: CPMG begun at ZPC after initial 180° pulse as described in the text. Open triangles and lower time scale: protein T_2, obtained by subtracting conventional CPMG asymptotic slope and its extrapolation to the starting time from the upper points. Open circles and lower time scale: the same subtraction using lower ZPC points. The ordinate is the accumulated integral over each signal gate period, expressed as total counts after A/D conversion.

Solutions in D_2O were prepared by first incubating the red cells in several changes of D_2O for from 24 to 48 h; solvent volumes were carefully measured, in order to calculate the amount of HDO signal expected. In this regard, it was assumed that 20% of the protein protons also exchanged for deuterons (Benson et al., 1973). Intermediate H_2O/D_2O mixtures were made by mixing the two extreme solutions.

Pulsed NMR relaxation measurements at 20 MHz and lower were made on a home-built spectrometer described elsewhere (Eisenstadt, 1980a). Details of T_1 and T_2 measurements are given in the next two sections, but common to both is the use of a full spin-echo train, called a CPMG sequence (Carr & Purcell, 1954; Meiboom & Gill, 1958), to monitor and distinguish the protein and water proton magnetizations. This consists of a 90° rf pulse, followed by as many as 8000 phase-shifted 180° pulses. Up to 256 arbitrarily selected echos can be individually monitored, by gating an integrator on 200-μs windows at the echo centers. Three 50-μs gates are also placed on the initial FID, to ensure that even those protein protons with a very fast T_2 are detected. These integrals are routed to a fast A/D converter, and then stored in a home-built microcomputer. Repeated measurements are accumulated for from 10 to 100 scans, to improve S/N. Then various curve-fitting programs are used to extract the component magnetizations, as described later.

T_2 Measurements

T_2 was measured by using the standard spin-echo CPMG technique as described above. Separation of protein and water components was based on the observation (most clearly seen in D_2O solution) that virtually all protein spins had T_2 values 2 orders of magnitude faster than the water protons. A typical result is shown in Figure 1, where a small amount of HDO solvent remained in the sample. a good two decades of log-linear data are present for a least-squaqres fit of the slow solvent component. Its T_2 is obtained, and its total amplitude as well, by extrapolation to zero time. Subtracting this from the full signal yields the protein T_2 decay, also shown in the figure, on an expanded time scale.

For dilute solutions in H_2O, an additional technique was useful in observing the protein signal above the solvent background. The method consists of initially inverting the total magnetization with an 180° pulse. When the z component of water magnetization (M_{Az}) has crossed zero (enroute from its initial value $-M_A^0$ to its equilibrium value $+M_A^0$), a CPMG sequence is begun. Only a signal due to the protein magnetization M_{Pz} is present; its amplitude is amost the full M_P^0, since protein protons relax much faster than water protons (next section). During the CPMG period, the protein T_2 decay is independent of any water decay (excluding for now the possibility of fast protein hydrogen exchange), and the further buildup of M_{Az} is irrelevant. Although the "zero point crossing" (ZPC) of the water M_{Az} is tied in a complex way to protein relaxation (eq 2), there always exists a unique time when $M_{Az} = 0$; we usually find it by trial, through observing an echo null on the oscilloscope.

Although protein T_2 is a distribution of values, it is needed for the interpretation of T_1 results, and of great interest in its own right. It should be noted that only a spin-echo experiment with closely spaced echos gives a true protein T_2. In principle, it is obtainable from the line widths of a FT spectrum (Sykes et al., 1978), but in Hb solutions, it would be all but impossible to distinguish chemical shifts and J splittings of overlapping lines from the true single line widths, even at the highest frequencies. Spin echos cancel the chemical shift and J splitting due to unlike nuclei; if the echo spacing is closer than the reciprocal J splitting due to like nuclei, it cancels that as well (Freeman & Hill, 1975).

The most clear-cut spin accounting is done with T_2 data, since unlike T_1, signal amplitudes do not depend on spin exchange. The protein and water amplitudes always agreed with stoichiometry to within 5% or better, which shows that we are observing all of the protein spins (i.e., there are none with T_2 of 100 μs or less) and that hydrogen atomic exchange is less than 5% in the time of a water T_2, typically 100 ms or so. If there were appreciable exchange, the amplitude of the slow component would be enhanced, according to eq 4d. However, even 1% or less exchange could still have an important effect on water T_2 (see Discussion).

One caution for quantitative measurement should be mentioned. For T_2 slope determinations (Figure 1), the correct base line to use is the final asymptotic echo amplitude, which is rarely zero because of pulse imperfections (Vold et al., 1973). For this purpose, we subtract the $(n + m)$th echo from the nth echo, for all n echos up to half-way through the echo train. Generally m is chosen large enough to be in the base-line region, but even if a significant signal remains at the mth echo, it can be shown (Eisenstadt, 1980c) that if the decay consists of one or several exponentials, this "early subtraction" will still give the correct slope(s). But the absolute values of M_P^0 and M_A^0 are the echo amplitudes extrapolated to zero time, relative to the true electrical zero. We therefore intersperse data taking with occasional runs with no sample and subtract these from the T_2 raw data. This also eliminates the effect of FET switching transients and proton signals from supporting structures, of some importance for exhaustively deuterated samples.

Both protein and water T_2 values are diagnostic of sample defects. When Hb denatures, the protein T_2 distribution is greatly enhanced in the region of 10–100 ms, because the

greater flexibility of the polypeptide segments leads to line narrowing (MacDonald & Phillips, 1969). The water T_2 is a sensitive indicator of metHb formation. We measure the water T_2 with great accuracy using two decades of decay; this value is then used for extraction of the water component in T_1 experiments (see below). Finally, the protein T_2 can give a rough indication of the spin-diffusion constant, to verify good protein spin mixing (Eisenstadt, 1981).

T_1 Measurements

T_1 was measured by using a conventional inversion technique, as well as a method which suppresses the water phase, described later. In both methods, the recovery of $M_z(t)$ from the excitation at $t = 0$ was monitored with a short CPMG sequence, 30–300 echos (depending on the magnitude of the water T_2) and several gates on the initial FID. The various delay times at which recovery was sampled were automatically stepped by the computer, and at the end of each sequence of delays, an echo train was taken with no excitation; this provided a continuous monitoring of the equilibrium magnetization, which was digitally subtracted from the other scans. Thus, the differences from equilibrium, $\Delta M_z(t) = M_z(t) - M^0$ for each channel, are stored in computer memory.

The echo spacing and number were chosen such that the last 10 or more echos were entirely due to the water phase; this is possible due to the short protein T_2. By use of the accurately known water T_2 from the CPMG experiments described above, the value of $M_{Az}(t)$ for the water phase alone is obtained by extrapolation back to the start of the CPMG sequence. The relaxation of protein protons alone are then obtained by subtracting these extrapolated water values from the FID and early echo signals.

In addition to the separation of components, the use of a long echo train greatly enhances S/N in a T_1 experiment, compared with monitoring recovery simply with an FID. This points out the fallacy in the common belief that T_2 measurements are inherently more efficient than T_1. If the T_1 monitoring echo train is stretched for as long as T_2 allows, say some hundreds of echos, then each T_1 data point is more than 10 times as precise as each T_2 (single echo) data point. We typically do 100 repetitions for T_2 runs, 10 for T_1, and could probably do with fewer. At any rate, when $T_1 \neq T_2$ (usually true in biological systems), both should be measured whenever possible.

For solutions in H_2O, the protein signal is difficult to measure in the presence of the large solvent signal, and a selective excitation scheme (denoted WS) was used on the basis of the enormous difference in protein and water T_2 values (Eisenstadt, 1980c). An initial pulse triplet, comprising a 90° rf pulse, a (−180°) pulse at time $\tau/2$, and a second 90° pulse at time τ, is applied. The first pulse turns the total equilibrium magnetization M^0 into the x–y plane (M_{xy}), the second pulse refocuses that portion of M_{xy} lost through coherent dephasing phenomena such as static field inhomogeneities or chemical shifts, and the final 90° pulse restores M_{xy} to the $+z$ direction. During τ, M_{xy} has decayed due to incoherent processes. From the known T_2 values, choosing a τ of a few milliseconds means that virtually all of the water signal is restored to the z direction, but most of the protein signal has decayed to zero. The precise value of the latter can be read off the measured protein T_2 distribution, e.g., Figure 1. After the second 90° pulse, the delays and monitoring sequences proceed as for the inversion experiment. The initial values to use in eq 1 for a WS T_1 experiment are thus $M_{Az}(0) - M_A^0 \approx 0$ and $M_{Pz}(0) - M_P^0 \approx M_P^0$. A WS experiment also gives the clearest measure of spin transfer between protein and water spins, since the initial spin-temperature difference is maximized. S/N is inherently poorer than for the inversion method, since subtraction of large signals is involved. A stacked plot illustrating this selective T_1 technique was shown as Figure 1 of Eisenstadt (1981).

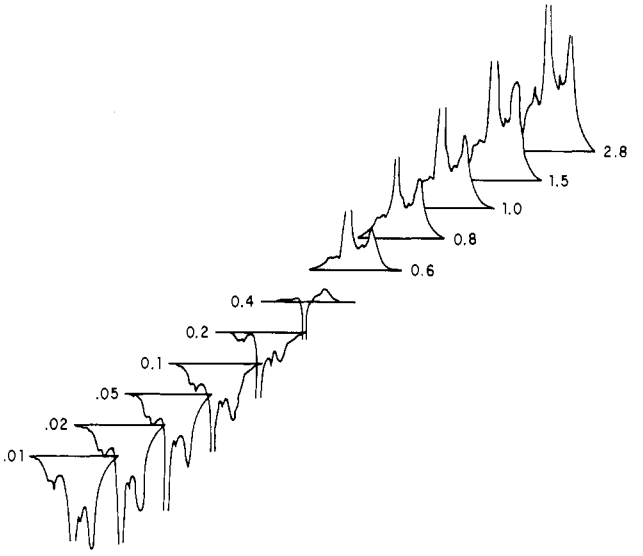

FIGURE 2: Hb spectra at various delay times after an initial inverting pulse. Data taken at 200 MHz, 20 °C, with 5.0 mM sample in 70% H_2O. The aliphatic protons are the large upfield peak (to the right) and were used to monitor protein T_1. The large water peak is off scale.

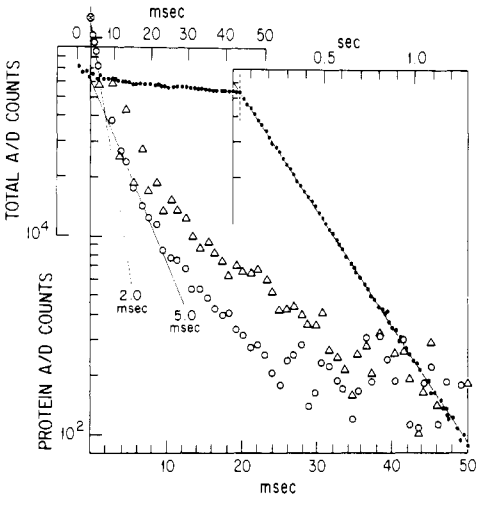

FIGURE 3: Spin-echo data for 4.0 mM Hb in H_2O at 24 °C, 20 MHz. Data display as in Figure 1 but ZPC echos not shown. Subtracted protein signals are relatively smaller than in Figure 1 and use the inner ordinate scale. Tangents to ZPC protein data are drawn from the 100% and 50% initial amplitudes, with slopes as shown, in milliseconds.

Data at 100 and 200 MHz were taken with JEOL 100 and Varian 200 spectrometers. Only T_1 was measured and only for a single set of 5.0 mM Hb solutions in various H_2O/D_2O mixtures. Spectra were observed at about seven delay times following an inverting pulse. Figure 2 shows a 200-MHz result for Hb in a 50% H_2O/D_2O solvent. We used only the broad aliphatic peak to monitor recovery.

Data Analysis

Figures 3 and 4 show data for a single sample, 4.0 mM Hb in 100% H_2O at 24 °C and 20 MHz. We present the analysis in great detail, to validate the two-phase exchange formalism, eq 2–4, and show how the fundamental relaxation parameters R_{1p}, R_{1a}, k_s, and k_t are extracted. Particular attention was paid to comparison of signal amplitudes among the four types

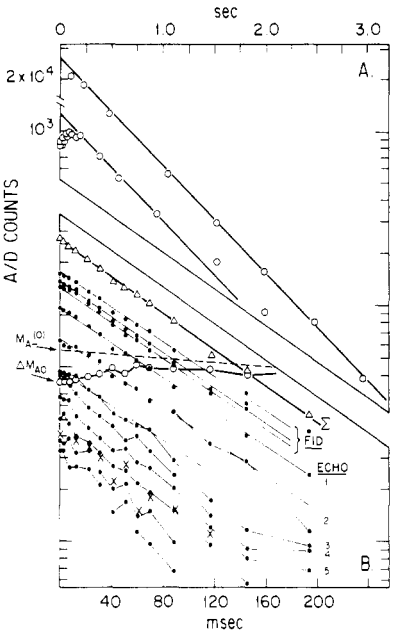

FIGURE 4: T_1 data for 4.0 mM Hb in H_2O at 24 °C, 20 MHz. (A) Upper circles: T_1 recovery of water protons alone, after a conventional inverting 180° pulse. Lower circles: water recovery after excitation by a WS 5 pulse triplet. (B) Protein T_1 after WS 5 triplet excitation. Points show recovery monitored by individual FID and echo gates; points for late echos are connected, for distinguishability. Upper triangles: protein recovery monitored by the sum of all FID and echo gates. Circles: water recovery [an expansion of lower data in (A)]. Crosses: Fast component of water recovery, as described in the text.

of experiments. This aspect has been underexploited in NMR work but can yield good quantitative analysis when measured side-by-side with well-defined standards.

The upper data and time scale of Figure 3 show a standard CPMG experiment; after the first 50 echos, data were collected only for every 20th echo, hence a change of time scale. The water T_2 can easily be followed for two or more decades; a least-squares fit of this log-linear portion is then subtracted from the early echos to yield the T_2 distribution of the protein protons. These are shown as triangles, for the lower time scale. They result from the subtraction of two large quantities; hence, inaccuracies proportional to the total signal are greatly magnified, e.g., the low signal from the first few odd echos (Vold et al., 1973). A more accurate protein T_2 is obtained by eliminating the water signal, the ZPC method described above. The small residual water signal in the ZPC experiment is subtracted by using the accurately known slope from the standard CPMG experiment, yielding the circles on the lower portion of Figure 3. The shape is the same as for the triangles, but with less scatter. But the overall amplitude of the protein T_2 in a ZPC measurement is about 20% lower than that of a standard T_2 measurement, as shown. This is a direct measure of k_t, as discussed later.

The relative amplitudes of the water and protein components are in good agreement with the spectroscopic Hb determination. By use of a molecular weight of 64 400, a protein specific volume of 0.75, and 4664 protons per Hb tetramer, for this 4.0 mM solution, the Hb and water proton molarities are 18.6 and 89.5 M/L. These mole fractions of 0.172 and 0.828 compare well with the amplitudes of the two components extrapolated to zero time, fractional values 0.205 and 0.795. Corrections to the CPMG data of Figure 3 are as described under Experimental Procedures. Even the absolute values are useful and agree with the signal from an equal volume of Ni-doped water, with proton molarity of 111 M/L. Thus, we have confidence that all protein protons are being observed.

To compare the protein T_2 values at different frequencies or other parameters, we characterize the distribution by an initial slope, and the slope of the tangent drawn to 50% of the initial amplitude, as shown in Figure 3. This is important, for example, to see if all T_2 values simply scale with viscosity, or if more subtle effects are involved (see Discussion).

Figure 4A (upper data) shows a conventional inversion–recovery T_1 experiment for the water protons alone, extracted as described under Experimental Procedures. This yields the most accurate value of ϕ_{1-}, the slow exponential decay rate of eq 2b. The amplitude of the water signal agrees well with the T_2 result above. In this experiment, data at times less than 100 ms were not taken. When they were, the water signal in an INV experiment shows an initial flatness due to rapid spin exchange with the protein protons. Spin exchange is more accurately measured by selectively exciting the protein spins and monitoring the amounts transferred to the unexcited water. This is shown in the lower half of Figure 4A and the early points on the expanded scale of Figure 4B. The recovery of the protein spins after selective excitation is also shown in the latter. To demonstrate the rapid spin mixing and equilibration of protein protons, we show the T_1 recovery as monitored by the individual FID and echo gate signals, up to echo 8 (7.7 ms after 90° pulse). Although scatter is large when examined gate by gate, we can see no indication of an initial induction period, where protein spins begin their local equilibration at different rates (clearly seen in the D_2O solutions described below).

The most accurate value of ϕ_{1+}, the fast relaxation rate in eq 2a, is obtained by integrating the entire protein signal, FID and echo gates, shown as the triangles in the upper part of Figure 4B. We also plot (not shown here) the recovery of the protein amplitude extrapolated to the start of the monitoring CPMG sequence; this is equivalent to the integral of the entire frequency-domain protein spectrum. Its value immediately following the selective pulse triplet, ΔM_{P0}, is needed to obtain k_s, below, and agrees with the magnitude predicted by the protein T_2 of Figure 3. Its variation with recovery time, $\Delta M_P(t)$ is that predicted by eq 2a. For selective protein excitation, the slow protein component $M_{P-} \exp(-\phi_{1-}t)$ is negligible (ΔM_{A0} small; eq 4b), so the data of Figure 4B is purely $M_{P+} \exp(-\phi_{1+}t)$.

In WS experiments, the initial value ΔM_{A0} is always finite, due to imperfect rf triplet pulses, but so long as it is small, it does not interfere. There are only a few data points for the slow asymptote M_{A-}, but its slope is accurately known from the INV experiment, so the water relaxation may be decomposed into its M_{A+} and M_{A-} components, as shown. In principal, ϕ_{1+} can be determined from the water fast component also, but there is not enough signal (i.e., spin transferred) for much accuracy. It agrees reasonably with the protein fast component (Figure 4).

By observing the protein T_1 via the individual FID and echo gates in a WS experiment, one also obtains the most graphic demonstration of rapid protein spin mixing. It is particularly apparent when the solvent is mainly D_2O, since the protein component of distant echos can be measured. Figure 5 shows the protein relaxation following an excitation triplet with τ = 5 ms, with useful recovery signal out to echo 16 (about 15 ms from the 90° pulse). The FID signals (upper three decays) and the first few echos have a faster recovery than the other echos for about 20 ms; thereafter, they are parallel. By contrast, late echos show an initial flatness for about 20 ms. This is because for a 5-ms triplet, those protons with a long T_2 (such as those of flexible side chains) will have most of their

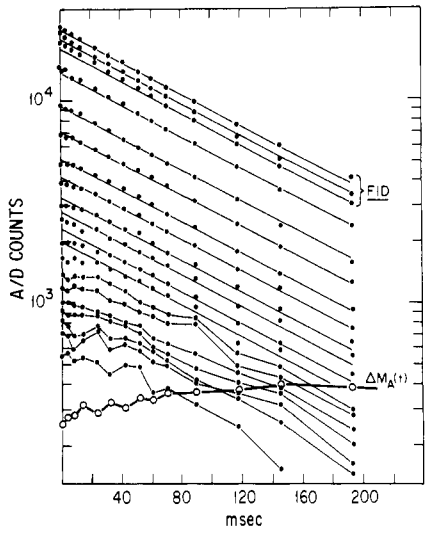

FIGURE 5: T_1 recovery of protein protons after a WS 5 triplet excitation for 3.6 mM Hb in 95% D_2O at 25 °C, 20 MHz. Points show recovery monitored by individual FID and echo gates, up to echo 16. The early part of the recovery of residual HDO protons is shown as circles. Noisy data points are connected for distinguishability.

equilibrium magnetization restored at the end of the triplet. Thereafter, they share it with the ones with short T_2 values (such as the more rigid backbone protons); until after 20 ms, they all recover as a unit. At 37 °C, the same effects were observed out to echo 36. In H_2O, this initial equilibration has always seemed much faster (Figure 4), although poorer S/N precludes following it in such detail.

The magnetization transferred to the water spins in a WS experiment measures k_s directly. First, the amplitude of the slow water component, M_{A-}, is derived from the lower data points in Figure 4A by extrapolation to zero time. Although the signal is small and the data points few, their slope must be the same as in the INV experiment above, which is known accurately; this slope is then input as a constrained parameter in a nonlinear least-squares fit of the lower $\Delta M_A(t)$ data to two exponentials. The amplitude M_{A+} from this fit and the quantities ΔM_{P0} and ΔM_{A0} derived from Figure 4B are then used in the approximation of eq 4c

$$(\phi_{1+} - \phi_{1-})M_{A+} \approx -k_s\Delta M_{P0} \quad (5)$$

to obtain k_s. A more refined value could now be obtained by using the first term of the right of eq 4c, but experimental accuracy rarely warranted this. The inverse transfer rate, k_t, follows from detailed balance, $N_P k_s = N_A k_t$.

The remaining two unknowns, R_{1p} and R_{1a}, can now in principle be found by exact solution of eq 3 for ϕ_{1+} and ϕ_{1-}, but it is simpler to use an iterative procedure, starting with the approximate formulas

$$\phi_{1+} \approx R_{1p} + k_s + k_s k_t/(R_{1p} - R_{1a} + k_s - k_t) \approx R_{1p} + k_s \quad (6a)$$

$$\phi_{1-} \approx R_{1a} + k_t - k_s k_t/(R_{1p} - R_{1a} + k_s - k_t) \approx R_{1a} + k_t \quad (6b)$$

In most cases, R_{1p} was so large that the first approximation was accurate enough.

These approximations also have a deeper meaning. For highly dilute protein solutions in H_2O, k_t is negligible, and the last form of eq 6a becomes exact. Qualitatively, it means that such an excess of water protons becomes an infinite sink for magnetization, regardless of the intrinsic R_{1a}. In a red cell experiment such as described above (Eisenstadt & Fabry, 1978), we could have seen the same k_s whether the extracellular water was doped with Mn or not; the presence of Mn simply made it easier ro observe the protein protons, by making $R_{1p} \ll R_{1a}$. Similarly, for the case of a highly deuterated solvent, k_s is near zero, and the slow component is exactly $R_{1a} + k_t$; i.e., the protein protons are an infinite sink.

Two final verifications of the two-phase exchange scheme can be demonstrated, since, in principle, the set of parameters is overdetermined by two. These last quantities are of limited accuracy but are an independent qualitative check. The fast water component in the WS experiment, $M_{A+}\exp(-\phi_{1+}t)$, is obtained by subtracting the slow water component, and is shown by crosses in Figure 4B. Its slope is consistent with the protein fast component.

The protein T_2 data points of the ZPC and ordinary CPMG experiments (Figure 3) differ because of the second, k_t term on the right side of eq 4b. For the INV experiment, ΔM_{A0} is now the full water signal $2M_A^0$, and there is a relatively large M_{P-} term. Qualitatively, after the 180° pulse, most of the protein magnetization decays rapidly, at the rate ϕ_{1+}, but thereafter, a small residue remains, which is transferred slowly from the water spin system. By use of all of the known quantities in eq 4b, at a time of 409 ms, a difference of 2000 A/D units between the two protein T_2 curves is calculated. This approach has the potential to give an independent measure of k_t, but we did not pursue it.

Data in 95% D_2O show some qualitative differences. The much-reduced water signal allows the protein relaxation to be measured with considerable accuracy. We show experiments analogous to those described above. In Figure 1, the protein T_2 values derived from a standard and a ZPC CPMG experiment agree closely, since the M_{P-} term is negligible (ΔM_{A0} small now). There are enough residual solvent protons to accurately measure T_2 of HDO. From its amplitude extrapolated to zero time, using the known Hb concentration of 3.6 mM, a solvent proton fraction of 0.040 is calculated.

The conventional INV T_1 experiment for HDO relaxation (not shown) yields straightforward single exponential behavior; as expected, it is about twice as slow as the equivalent H_2O experiment, since the large contribution of the intramolecular proton is gone. The early stages of HDO relaxation in a WS experiment are shown in Figure 5; it is qualitatively the same as in H_2O (Figure 4B). Although the total spin transferred to the protein is now small, the amount transferred per water proton is little changed, since only 20% of the protein protons have exchanged for deuterons; this is the quantity measured by the $\Delta M_A(t)$ data.

The most interesting difference from behavior in H_2O is shown by the protein relaxation in the WS experiment (Figure 5) where the T_1 behavior of a large number of individual echos can be accurately followed. An initial induction period is evident, with the FID and first echo showing a slight upward curvature and late echos a pronounced downward one. This would arise if there were selective excitation among the protein spins themselves, as indeed the protein T_2 predict. By use of Figure 1, for a WS5 experiment, protein protons with a T_2 of 5 ms would only be 37% excited and would pick up "saturation" from any neighboring spin with a much shorter T_2. After about 20 ms, the protein spins appear well mixed and relax as a unit, with ϕ_{1+}^{-1} of 95 ± 4 ms.

RESULTS

Figure 6 shows the Hb protein proton T_2 and the measured fast rates ϕ_{1+}, which are largely R_{1p}. Four protein concentrations were used in each of two extreme solvents, 100% H_2O and about 95% D_2O (the latter is imprecise due to experimental mishap). Measurements were made at 25 °C at 5, 10,

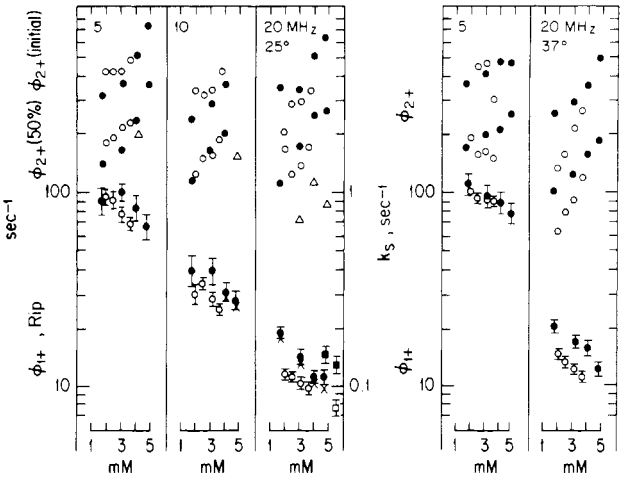

FIGURE 6: Protein ϕ_{1+}, ϕ_{2+}, R_{1p} and k_s, at three frequencies, two temperatures, and various concentrations. Spacing is such that when points of the same concentration are connected, this is also a plot vs. log frequency. Solid circles are data in 100% H_2O and open circles ca. 95% D_2O. ϕ_{2+} characterized by initial (100%) slope (uppermost group of circles) and 50% slope (next group). A few k_s values are shown as triangles by using the right ordinate of the 25 °C grouping. When subtracted from the solid circles with error bars, they yield R_{1p}, shown as (×). ϕ_{1+} values from earlier work with red cell suspensions are shown as analogous open and solid squares (see the text).

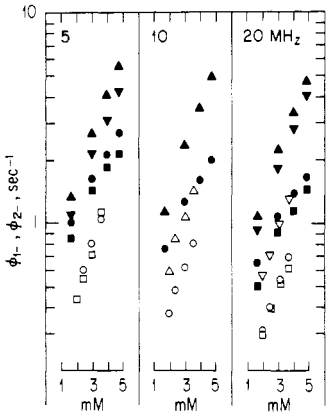

FIGURE 7: Water ϕ_{1-} and ϕ_{2-}, for the same samples as Figure 6 and plotted similarly. All solid symbols, H_2O; all open symbols, HDO. (●, ○) ϕ_{1-}, 25 °C. (■, □) ϕ_{1-}, 37 °C. (▲, △) ϕ_{2-}, 25 °C. (▼, ▽) ϕ_{2-}, 37 °C.

and 20 MHz and at about 37 °C at 5 and 20 MHz. The horizontal scale within each frequency domain of Figure 4 is in millimolar concentration units, but the overall spacing is such that, for a given concentration, the abscissa is also a log frequency scale, which greatly aids comparisons. As discussed, protein T_2 is a distribution of values, and we have characterized it by an initial slope and the slope of a tangent to the decay curve from 50% of the full ordinate (Figure 3). The quantities R_{1p} and k_s, derived from the data as described in the previous section, are also shown. A few ϕ_{1+} data from previous work with red cell suspensions (Eisenstadt & Fabry, 1978) are plotted as squares. Cells were shrunken and highly concentrated, in a $MnCl_2$ medium. The results for D_2O agree with the present experiments, but in H_2O they are significantly faster. For such high concentrations of Hb, the "infinite sink" approximation of eq 6a is no longer valid, and back-diffusion of spin via k_t is important.

Figure 7 shows the water relaxation for the same set of samples, plotted as in Figure 6. There is a steep primary dependence on Hb concentration. It is more useful to interpret the results on a per protein basis, and these are shown in Figure

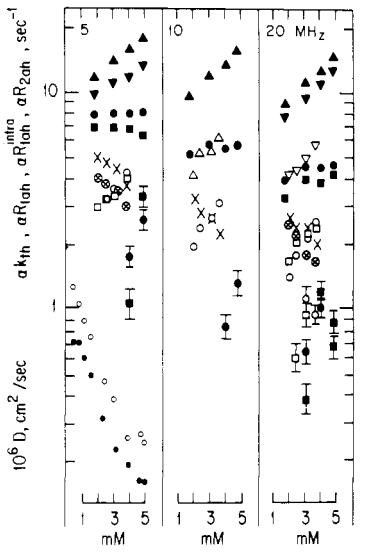

FIGURE 8: Water relaxation data of Figure 7, reduced to a per protein basis as described in the text (eq 14). Circles, squares, and triangles without error bars correspond to the same quantities as in Figure 7. αk_{th} values shown with error bars are for the following: (●) H_2O, 25 °C; (○) HDO, 25 °C; (■) H_2O, 37 °C; (□) HDO, 37 °C. αR_{1ah}(intra) are shown at (×) 25 and (⊗) 37 °C. For comparison, at the lower left, we show Hb diffusion constant measurements at (●) 25 and (○) 37 °C (Keller et al., 1971).

8, along with other derived quantities. Details of these separations are given under Discussion.

The general relaxation behavior observed at 10 and 5 MHz, 37 °C, and other Hb concentrations is similar to that illustrated by Figures 1–5. Protein T_1 varies sharply with frequency, water T_1 less so, and T_2 of both hardly at all. All quantities vary strongly with Hb concentration, but in different ways (see Discussion). One qualitative difference is that, at 5 MHz, the assumption of good protein spin mixing breaks down, and curvature of the sort seen in the early part of Figure 5 is now spread over the entire protein recovery curve. This is because T_1 approaches T_2 as the frequency is lowered, and the spin-exchange term is approximately $^2/_9\ T_2^{-1}$. The values shown for ϕ_{1+} and R_{1p} at 5 MHz are thus an average over some distribution of T_1 values, although the spread of values is still much narrower than that of T_2.

To test certain relaxation models, measurements were made on a series of 5.0 mM Hb solutions in H_2O/D_2O mixtures, at 20, 100, and 200 MHz. Figure 9 shows R_{1p}, R_{1a}, k_s, and several amplitudes at 20 MHz, derived from the data as described above; the decrease in protein signal of 20% due to 12 h of isotope exchange is apparent. At 100 and 200 MHz, water and the aliphatic proton peak were measured at various delay times following a 180° pulse. Their return to equilibrium amplitudes should be biphasic just as at 20 MHz, although for a simple INV experiment, the fast component of the water is small (see Figure 4). The protein recovery was clearly multiexponential, the more so the greater the H_2O content. These aliphatic and water data are shown in Figure 10.

Discussion

The relaxation phenomena shown above are almost certainly due to magnetic dipolar interactions between proton spins; a remotely possible quadrupolar mechanism is briefly considered below. Basic features of spin–lattice relaxation are well described by a two-phase spin-exchange model. Protein and water protons are considered as distinct phases, in each of which all spins are equivalent and have intrinsic relaxation rates R_{1p} and R_{1a}, respectively. Magnetization is also ex-

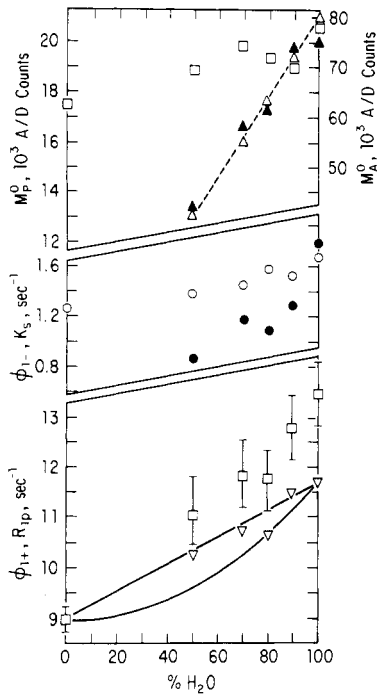

FIGURE 9: Relaxation data at 20 MHz, 25 °C, for 5.0 mM Hb in various H_2O/D_2O mixtures. Upper group: (□) total protein amplitude, from T_1 data; (△) total water amplitude, from T_1 data; (▲) the same, from T_2 data. Middle group: (○) ϕ_{1-}; (●) k_s. Bottom group: (□) ϕ_{1+}, from protein T_1 data; (▽) R_{1p}, from $\phi_{1+} - k_s$. Lines show possible linear and quadratic dependence of R_{1p} on H_2O fraction.

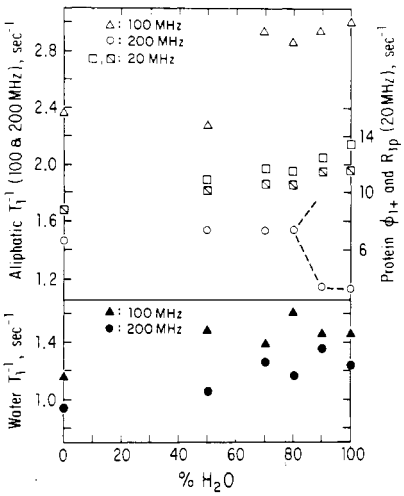

FIGURE 10: T_1 values of water and aliphatic protons for 5.0 mM Hb, 25 °C, in various H_2O/D_2O mixtures, from 100- and 200-MHz FT spectra. Values of ϕ_{1+} and R_{1p} at 20 MHz (right ordinate) are repeated from Figure 9, for comparison: (□) ϕ_{1+}; (⊠) R_{1p}.

changed between the two phases at their boundaries, at a rate k_s per protein proton and k_t per water proton; chemical equilibrium dictates $N_P k_s = N_A k_t$. The coupled rate eq 1 describing this have a solution of two exponentials (eq 2). In the previous section, we have shown the evidence for the validity of these solutions. The remaining problem is to explain R_{1p}, R_{1a}, and k_s (k_t) in terms of microscopic models for the spin interactions and their dynamics.

The results for the protein protons are the easier to understand. A protein spin has a magnetic dipolar interaction with its permanent neighbors leading to the relaxation formulas

$$R_{1i} = (3/10)\gamma^4\hbar^2\sum_j r_{ij}^{-6} f_1(\tau_c) \quad (7a)$$

$$f_1(\tau_c) = \tau_c(1 + \omega_o^2\tau_c^2)^{-1} + 4\tau_c(1 + 4\omega_o^2\tau_c^2)^{-1} \quad (7b)$$

$$R_{2i} = (1/20)\gamma^4\hbar^2\sum_j r_{ij}^{-6} f_2(\tau_c) \quad (8a)$$

$$f_2(\tau_c) = 9\tau_c + 15\tau_c(1 + \omega_o^2\tau_c^2)^{-1} + 6\tau_c(1 + 4\omega_o^2\tau_c^2)^{-1} \quad (8b)$$

$$R_{1ij} = (1/10)\gamma^4\hbar^2 r_{ij}^{-6}[\tau_c - 6\tau_c(1 + 4\omega_o^2\tau_c^2)^{-1}] \quad (9)$$

For exchangeable protein protons, these may or may not apply, depending on the lifetime for exchange; we consider this later. We follow the approach of Kalk & Berendsen (1976) and calculate relaxation from the pairwise interactions of spins. This is based on the Solomon formulas (Solomon, 1955) for relaxation of two spins at a fixed distance but randomly fluctuating orientation; however, here we have summed over all spin pairs (eq 7–9). Because of the strong r^{-6} dependence, only the near neighbors in methyl and methylene groups are explicitly calculated, and interactions with all other spins are approximated by integrating over a continuum, using a proton density of Hb of 4.1×10^{22} protons/cm^3, based on a specific volume of 0.71 mL/g (Tanford, 1961) and 4664 protons per Hb tetramer (*Merck Index*, 1968). For the hemoglobin equilibrated for 24 h in D_2O, this density is reduced by 20%.

The methyl protons are given a special mechanism due to internal rotation with an assumed correlation time τ_r of 10^{-10} s (Kalk & Berendsen, 1976), much shorter than τ_c of overall Hb tumbling, 10^{-7} s (Hallenga & Koenig, 1976). The expression for R_1, for each of two interactions, is

$$R_{1CH_3} = (3/10)\gamma^4\hbar^2 r^{-6}[(1/4)f_1(\tau_c) + (3/4)f_1(\tau_{c3})] \quad (10a)$$

$$\tau_{c3}^{-1} = \tau_c^{-1} + \tau_r^{-1} \quad (10b)$$

Thus, at frequencies higher than 100 MHz, relaxation due to rigid-body tumbling is negligible, and methyl protons act as relaxation sinks for the entire protein proton system; these in turn provide the sole relaxation pathway for water protons, via spin transfer at the interface. But in the 5–20-MHz range the opposite is true, and internal rotation contributes only a small, frequency-independent term. Nevertheless, methyl (and methylene) protons still make a large contribution to overall relaxation because of the short intragroup distances, assumed 1.8 Å. In Table I we show the contributions to relaxation of the methyl and methylene protons at various relevant frequencies. For neighboring protons at distances of 2.8 Å and further, the contribution to relaxation is taken as

$$R_{cont} = (3/10)\gamma^4\hbar^2 f_1(\tau_c)(4\pi n/3)(b_1^{-3} - b_2^{-3}) \quad (11)$$

That is, for a sphere of radius $b_2 = 27$ Å, R_{cont} depends only on b_1, the distance of closest approach, 2.8 Å. This term is shown in column 5, again with a τ_c of 10^{-7} s. The same spherical integral is used even for protons near the surface; this probably contributes little error, due to the insensitivity to b_2.

The measured R_{1p} will be the weighted average over all spins. The continuum contribution is added to the methyl and methylene spins, columns 3 and 4, and is the sole term for other all other spins. For fully protonated Hb (in H_2O), there are 1134 methyl, 1148 methylene, and 4664 total protons; thus

$$R_{1p}(H_2O) = 0.246R_{1CH_2} + 0.243R_{1CH_3} + 0.511R_{1cont} \quad (12)$$

Agreement with the measured R_{1p} for 5 mM, 25 °C, at 5 MHz is fairly good (Figure 11), considering that only a rough average τ_c of 10^{-7} is used, but the calculated value is about 50% too slow at 20 MHz. It is quite likely that other internal motions in addition to methyl rotation are beginning to contribute here, via correlation times shorter than rigid tumbling;

Table I: Calculation of Protein Proton Relaxation in Hemoglobin, As Described in the Text

Larmor freq $\omega_o/2\pi$ (MHz)	H_2O					D_2O				
	f_1	R_{1CH2} (s^{-1})	R_{1CH3} (s^{-1})	R_{1cont} (s^{-1})	R_{1p} (s^{-1})	f_1	R_{1CH2} (s^{-1})	R_{1CH3} (s^{-1})	R_{1cont} (s^{-1})	R_{1p} (s^{-1})
200	1.27×10^{-11}	0.102	4.10	0.034	1.04	1.02×10^{-11}	0.079	4.08	0.022	1.26
100	5.06×10^{-11}	0.408	4.30	0.136	1.21	4.08×10^{-11}	0.307	4.23	0.088	1.38
50	2.03×10^{-10}	1.63	5.12	0.545	1.92	1.63×10^{-10}	1.22	4.81	0.349	1.97
20	1.25×10^{-9}	10.0	10.7	3.29	6.74	1.02×10^{-9}	7.70	8.48	2.20	5.80
10	4.99×10^{-9}	40.2	30.8	13.4	24.2	4.06×10^{-9}	30.5	29.9	8.72	21.9
5	1.91×10^{-8}	154	107	51.3	90.1	1.58×10^{-8}	119	101	33.9	80.7
2	9.34×10^{-8}	753	506	251	436	8.27×10^{-8}	623	405	178	384
1	2.27×10^{-7}	1829	1225	610	1059	2.22×10^{-7}	1665	1075	476	1025
0.5	3.78×10^{-7}	3042	2028	1013	1759	4.17×10^{-7}	3136	2020	896	1928
0.2	4.75×10^{-7}	3822	2501	1272	2198	5.76×10^{-7}	4337	2791	1237	2664
0.1	5.00×10^{-7}	4027	2688	1341	2329	6.10×10^{-7}	4590	2954	1310	2820

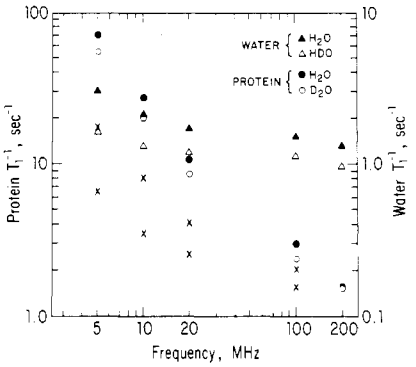

FIGURE 11: Complete frequency dependence of Hb and water T_1, for 5 mM Hb in 100% H_2O and ca. 95% D_2O, 25 °C. For frequencies of 20 MHz and lower, the data of Figure 6 were extrapolated to 5 mM. Water data with the 200-MHz value subtracted away are shown by (×).

hence, R_{1p} falls off less steeply than $(\omega_o^2\tau_c)^{-1}$.

In D_2O, at least three factors operate to change the overall R_{1p}. First, the relative fraction of CH_3 and CH_2 protons is larger than in H_2O, since they are nonexchanging. Assuming the full 20% of exchangable sites are deuterated (and are uniformly distributed over the protein volume)

$$R_{1p}(HDO) = 0.308R_{1CH_2} + 0.304R_{1CH_3} + 0.388R_{1cont} \quad (13)$$

Second, R_{1cont} is 20% smaller, since the proton density is reduced by exchange. Finally, the solvent viscosity at 25 °C is 0.895 (H_2O) and 1.113 (D_2O) (Nemethy & Scheraga, 1964). This appears to be the major factor explaining the smaller R_{1p} in D_2O. We have accordingly increased the value of τ_c by 24% in the calculation of f_1. Values are given in the last column of Table I.

The net effect is that the calculated $R_{1p}(D_2O)$ is about 10% smaller than $R_{1p}(H_2O)$ between 2 and 20 MHz, they are equal at 1 and 50 MHz, and $R_{1p}(D_2O)$ is about 20% larger at both high- and low-frequency extremes. Experimentally, we observe that $R_{1p}(D_2O)$ consistently is about 20% smaller between 5 and 100 MHz; at 200 MHz, they become qualitatively different (see below). Again, it seems likely that, above 20 MHz, local motions become important. It has been observed in ^{13}C relaxation studies (Jardetzky et al., 1980) that these motions are also sensitive to viscosity.

Two other isotope-dependent mechanisms should be considered. One is that the exchangable amide protons contribute greater than average values to overall relaxation. Winter & Kimmich (1982) have observed a cross-relaxation phenomenon involving the nitrogen spins, which manifests itself when the N quadrupolar splitting matches the proton frequency. They have observed dips in the curve of protein proton relaxation vs. frequency for solid albumin, but not in solution, where it is presumably averaged out due to tumbling. In any case, the dips occur at a frequency somewhat below our lowest value of 5 MHz. But the N–H interaction is distinctive in two other respects. The N–H distance is small, 1.02 Å (Winter & Kimmich, 1982); hence, relaxation is $(1.78/1.02)^6 = 28$ times more effective than for methyl proton pairs. But compensating this, the magnetic moment of ^{14}N is very small, which reduces the effectiveness by $(3.07/42.6)^2 = 0.0052$ compared to H–H interactions. The net effect is 0.146 times the methyl pair, so adding N–H terms to the calculations would contribute little.

The other possibility is that some fraction of H_2O is in intimate contact with the protein spin system for a time longer than R_{1p}^{-1}, so they are indistinguishable from protein spins, i.e., well mixed. Such rigidly attached protons could act as powerful relaxation centers; because of the short intramolecular water H–H distance of 1.51 Å (Lankhorst et al., 1982), this proton pair contributes 2.7 times more relaxivity than a methyl pair. But to explain the 20% discrepancy between H_2O and D_2O, an unreasonable number of tightly bound water protons would be needed, ca. 20% of N_P. Further, there is a simple test of this interesting mechanism through solvent isotopic dilution. As H is replaced by D, the number of H_2O molecules decreases quadratically with isotope fraction, and the difference between R_{1p} of H_2O and that of HDO would likely decrease even faster, since a rigidly bound HDO molecule probably contributes *less* than the average protein proton, because its nearest proton neighbor distance is 2.8 Å or greater. The net effect would be a steep initial decline of R_{1p} to some minimum and then a small increase to the limiting D_2O value, as the last HDO molecules are removed. Nothing of the sort is observed. Figure 9 shows R_{1p} for a 5 mM Hb solution at 20 MHz, 25 °C, and various H_2O fractions between 50 and 100%, as well as the limiting D_2O value. Within experimental error, the variation is linear with isotope fraction; so is solvent viscosity.

In contrast with protein solutions, this mechanism becomes very important in the spin equilibria of solid proteins and water (Shirley & Bryant, 1982). For lysozyme–D_2O at low temperatures, protein proton relaxation is determined entirely by methyl sinks, equilibrating with other protons via spin diffusion. At the same temperature in H_2O, relaxation is *slower*, due to the added burden of immobilized water spins. However, as the temperature is raised, the H_2O spins are become mobile, and hence effective relaxation sinks themselves, so the result is as described above, with $R_{1p}(H_2O)$ the faster.

We use a similar approach to estimate protein proton T_2 values (eq 8). For $\tau_c = 10^{-7}$ s, the first, frequency-independent

term dominates, and the second third terms are only significant at 5 MHz, where they contribute about 10% to the overall R_{2p}. Thus, in contrast to T_1, the slowest, rigid body τ_c will always dominate and can be taken as the correlation time for all nonexchanging spins. Nevertheless, there will be a distribution of T_{2p} values, since interproton distances vary. For methyl protons, the T_2 is not a simple exponential because of internal rotation (Kalk & Berendsen, 1976), but a small narrow component to the line width could never be observed. The broad component contributes 810 s^{-1}, the continuum 402 s^{-1}, giving a net of 1210 s^{-1}, or a methyl T_2 of slightly less than 1 ms. A similar R_2 obtains for methylene protons, and the remaining 50% of the protein protons would have an R_2 of about 400 s^{-1}. Looking at a typical protein T_2 measurement in D_2O (Figure 1), most of the spins appear to relax with a T_2 of between 1 and 5 ms, although a small but distinctly measureable fraction has much longer values.

Since R_2 depends linearly on τ_c and R_1 inversely, one also expects the opposite dependence on isotope fraction, i.e., all R_2 value about 20% faster in D_2O. Comparing protein T_2 distributions in H_2O and D_2O at the same temperature, concentration, and frequency, we find that both the initial slope and final asymptotic slope are about 10% faster in D_2O. The continuum term plays a greater role for T_2 than for T_1 and would be 20% smaller in D_2O, counteracting the effect of greater solvent viscosity. We cannot be any more quantitative than this.

Of greater interest are the relative changes in protein T_2 with concentration and temperature. If T_2 is solely due to rigid body rotation, then any variation would be strictly a viscosity effect, and the entire T_2 distribution would scale accordingly. This appears to be true; all T_2 data can be superimposed by expanding or contracting the time scale by a single multiplicative factor. This scaling effect has been exploited by de Witt et al. (1978) to detect the association of TMV subunits. The existence of viscosity scaling does not preclude the effect of faster local motions on T_2; as mentioned above, mobile side chains facing the solvent are also viscosity sensitive (Jardetzky et al., 1980).

The overall frequency dependence of R_{1p} is very steep (Figure 11), although not as steep as the ω_o^{-2} dependence predicted by simple theory (eq 7). Our frequency range is well above the center of the dispersion found in water relaxation studies or dielectric relaxation; for dilute Hb the center frequency would be about 1 MHz (Hallenga & Koenig, 1976) and, at our typical concentrations, even lower. Undoubtedly faster local motions are also playing a role and account for the gradual flattening at higher frequencies, even before methyl rotation begins to dominate. If this calculated methyl contribution is subtracted, the resulting frequency dependence is about $\omega_o^{-1.5}$.

At 200 MHz, R_{1p} is qualitatively different from that at lower frequencies. For 80% H_2O fraction or less, R_{1p} is independent of isotope fraction and follows a continuous curve with the lower frequency values. But for 100% H_2O, the aliphatic T_1 breaks into two components, indicating a strong spin-transfer term between water and protein spins. A possible indirect frequency dependence of the spin-transfer mechanism is discussed at length, in connection with the water T_1, where spin transfer plays a more important role.

Water Relaxation

Both R_{1a} and R_{2a} have a steep primary dependence on protein concentration (Figure 7), and it is more important to look at these rates on a per protein basis (Figure 8), since the goal is a microscopic model of relaxation per protein molecule. We therefore express these rates as

$$R_{1,2a} = (V_P/V)(1 - V_P/V)^{-1}\alpha R_{1,2ah} + [1 - (1 - \alpha)(V_P/V)](1 - V_P/V)^{-1}R_{1,2af} \quad (14)$$

The form of eq 14 is suggested by a simple fast-exchange model, where water is exchanging rapidly between the bulk solvent with relaxation rates $R_{1,2af}$ and a hydration region with rates $R_{1,2ah}$. The latter volume is taken proportional to the protein volume via a constant α. But the formula is really of greater generality, provided one refrains from grandiose interpretations of α. A minor exception is made in the second term, where a volume αV_P is excluded from the bulk solvent volume V_W, taking $\alpha = 0.2$ (Kuntz & Kauzmann, 1974). But the entire contribution of this term is really quite small. The values of R_{1af} used were 0.30 (H_2O, 25 °C), 0.21 (H_2O, 38 °C), 0.16 (HDO, 25 °C), and 0.12 (HDO, 38 °C) (Lankhorst et al., 1982; Hindman et al., 1973), and $T_{1af} = T_{2af}$ is assumed. Protein volumes are obtained from the measured concentrations by using a specific volume of 0.75 cm^3/gm (Bernhardt & Pauly, 1975).

We have determined R_{1a} in H_2O and 95% D_2O at 25 and 37 °C, at a range of Hb concentrations between 2 and 5 mM and at Larmor frequencies from 5 to 200 MHz. Even qualitatively, there is no coherent molecular picture that will encompass all of these results. A fundamental enigma of water relaxation has persisted since the earliest experiments almost 20 years ago (Koenig & Schillinger, 1969). That is, how does the water sense the protein tumbling motion, such that its T_1 frequency dispersion matches the protein dielectric relaxation dispersion and, from the results shown in this paper, the protein proton T_1 dispersion as well?

From the wide frequency dependence of Figure 11, it is seen that in the range above 5 MHz, R_{1a} has a much smaller frequency dependence than R_{1p}. This is mainly because R_{1a} approaches a high-frequency asymptotic value quite different from the pure solvent T_1. This value has the primary concentration dependence, and it has been speculated (Hallenga & Koenig, 1976) that it corresponds to a plateau region before a small, very high frequency dielectric dispersion. This seems plausible, since the low-frequency T_1 dispersion mimics the dielectric analogue so well. It is unfortunate that this has not been studied further, since NMR spectra can be taken at 500 MHz today, and water relaxation measurement would be trivial. The so-called dielectric δ dispersion (Hasted, 1973) occurs between 500 and 2000 MHz and is ascribed to the bulk of the water in the hydration layer, with lifetimes much shorter than 10^{-7} s but much longer than the free water diffusion jump time of 10^{-11} s.

We will ignore this asymptote in what follows, but if quantitative interpretation of our water data should be made, the high-frequency background must be substracted. We do this crudely in Figure 11, where the 200-MHz rates are subtracted from the others. The water R_{1a} dispersion becomes much steeper but still not as steep as the R_{1p} data.

Interpretation of water relaxation is further complicated by the sharply differing behavior of intra- and intermolecular dipolar relaxation in H_2O solutions. Due to the short intramolecular proton distance of 1.5 Å in the water molecule, the interaction of this proton pair dominates in H_2O, although the intermolecular contributions of all other spins is by no means negligible. Even in pure solvent, a simple calculation shows that about half of the relaxation is due to the molecular pair and half to all the other protons (Abragam, 1961). In fact, comparing our H_2O and HDO data under the same physiochemical conditions, both T_1 and T_2 differ by about a factor

of 2 for the two solvent species, at all frequencies, temperatures, and concentrations.

We first discuss HDO relaxation. For T_2 relaxation, one expects $R_2 \propto \tau_c$, with some slight frequency dependence at 5 MHz. Our HDO T_2 data are very incomplete, but for 20 MHz at 37 °C and 10 MHz at 25 °C, there is a steep dependence on protein concentration (Figure 8), even after reducing it to a per protein basis. This strongly suggests a viscosity-dominated effect.

The corresponding R_{1a} data are more complete. A tumbling τ_c dependence would be proportional to $(\omega_o^2\tau_c)^{-1}$, and in ratio $\omega_o^2\tau_c^2$ with R_{2a}. Assuming a τ_c of 10^{-7} s, R_2/R_1 is calculated as 158 at 20 MHz and 9.9 at 5 MHz. In contrast, the measured R_1 and R_2 differ by little more than a factor of 2 at either frequency. Furthermore, the concentration dependence of R_{1a} and R_{2a} are roughly parallel, suggesting the same linear τ_c dependence for both. This would occur if the main T_1 mechanism for HDO is via transfer of magnetization to the protein spins, since $k_t = (2/9)R_2$ at frequencies above τ_c^{-1} (Kalk & Berendsen, 1976). But several features show that this could not be the entire explanation. The frequency dependence of R_1 is more pronounced than for R_2 and would be larger still if we could separate out the high-frequency asymptote. The most unusual feature is the almost total lack of temperature dependence of R_{1a} (both at 5 and at 20 MHz), despite a 50% change in solvent viscosity from 25 to 37 °C. Almost any motional effect will have a shorter τ_c at higher temperatures.

Fortunately, the selective excitation (WS) experiments give a direct and independent measure of k_t. Although this is the least accurate of all derived quantities, we find that, for HDO, k_t is close to the value $(2/9)R_2$ predicted by simple dipolar theory. We also find that k_t of HDO and that of H_2O are about the same, as expected. Less certain, the temperature and concentration dependence of R_t seem parallel to those of T_2 for HDO. Then if we assume that $k_t = (2/9)R_{2a}$ rigorously for HDO and subtract it from the measured ϕ_{1-}, we are left with a residual R_{1a} of about the same magnitude and concentration dependence as k_t, and little or no temperature dependence. This is quite likely the high-frequency term discussed above. If its dispersion is above 200 MHz, then its relaxation rates would be of the form $R_1 = R_2 = A^2\tau_c$, a similar linear τ_c dependence as the 20-MHz R_2, but of course a completely different τ_c.

All of this implies several, or a distribution of, correlation times for water relaxation, with a long τ_c cutoff being the tumbling τ_c of the Hb itself. For HDO, R_2 and k_t would be dominated by the latter, which seems true (the possibility that both are due to atomic hydrogen exchange is discussed below). R_{1a} is the most difficult to explain. It results from single-quantum transitions caused by the dipolar fields of protein protons. The concentration dependence implies it is of the form $A^2\tau_i$, i.e., $\tau_i \ll \omega_o^{-1}$, and certainly τ_i is much less than the tumbling time, 10^{-7} s. Since the dipolar interaction is so short range (r^{-3}), this suggests that τ_i is the lifetime of water in the first Hb hydration layer, in which case there is surely a wide range of τ_i values. If so, then the lack of temperature dependence of R_{1a}, or even opposite temperature dependence of R_{2a}, is very puzzling, since the lifetime will surely decrease with increasing temperature. Also, such short-range motions "transverse" to the protein surface are unlikely to depend on long-range viscosity effects, as the concentration dependence seems to imply.

These inconsistencies lead one to suspect long-range effects. As noted above, the combined interaction of all intermolecular protons can account for half of the total relaxation in pure water, so one might expect a dense distribution of protein protons in the 1–5 mM range to do as much or more. For example, at 5 mM, the distance between 31 Å radius Hb spheres arranged in a simple cubic lattice is only 65 Å along the edge, i.e., almost touching. Decreasing the concentration by 10 (quite dilute by NMR standards) would only increase the spacing by the cube root of 10. The water geometry could be almost considered cagelike, surrounded by eight hemoglobins on average, with the farthest distance from a Hb being 55 Å (along the diagonal) and the average distance closer to 40 Å. With such intimate contact, hydrodynamic interactions could play a decisive role, as has been suggested (Koenig, 1980). Hydration water several layers deep could follow the tumbling motion of the Hb, in the classical viscous drag sense. A component of motion opposite to Hb tumbling can also be predicted from conservation of angular momentum considerations. Finally, the Hb molecules are so close that rapid water diffusion could cause a water molecule to experience rapid reversals of hydrodynamic velocity. Deeper consideration of such complex phenomena are far beyond the scope of this paper.

Water proton relaxation in H_2O is caused by all of the HDO mechanisms discussed above, plus the interaction with the intramolecular proton. The latter contribution is extracted by subtracting the measured HDO rates from the H_2O rates at the same physiochemical conditions and frequencies, with the following provisos: (1) solvent viscosity is 24% less in H_2O; (2) easily exchangable protein H sites will now be protonated. For the first, those contributions to relaxation which depend on water or protein tumbling via the first power of τ_c will be reduced 24%. From the above discussion, most of the HDO relaxation appears to have this dependence, so we assume the intermolecular rate of H_2O relaxation is 76% of the HDO value. The second effect is difficult to assess, since the location and lifetime of exchangeable protein protons is certainly varied and mostly unknown. Since there are 20% more protein protons in H_2O, we will assume that k_t and R_{1a}(inter) are enhanced by 20%. The net effect is that (1) and (2) tend to cancel.

Thus, we take the intramolecular relaxation to be simply the difference between the HDO and H_2O data, shown as crosses in Figure 8. Since the total $\alpha R_{1ah}(H_2O)$ shows almost no concentration dependence, then αR_{1ah}(intra) has a steep inverse concentration dependence, which is much like the protein R_{1p} and which suggests a $(\omega_o^2\tau)^{-1}$ dependence. αR_{2ah}(intra) is derived similarly (not shown). For the Hb tumbling τ_c of 10^{-7} s, R_2/R_1(intra) would be 158 at 20 MHz, but the measured ratio is about 2. Since the interaction strength is fixed by the well-defined geometry for the intra term (possible effects of water proton exchange are discussed below), the protein can only take affect through τ_c, i.e., hindering the free tumbling of the water in some way. Thus, in principle, R_2/R_1(intra) is independent of the interaction strength and provides the most direct measure of the correlation time of water relaxation. From the 2 mM 20-MHz data, we derive $\tau_c = 6.1 \times 10^{-9}$ and from the 5 MHz data, 1.6×10^{-8}, which is absurd. This is further strong evidence that τ_c is a distribution of values. In a similar vein, one can use the known interaction strength of two water protons at a distance of 1.5 Å and derive α. It is about 0.007 and frequency dependent. Similar low values are derived when simple two-state models are applied to frequency dispersion data (Hallenga & Koenig, 1976).

Then it is difficult to understand the steep concentration dependence of αR_{1ah}(intra), since the water lifetime in a single layer should not depend on long-range influence from a neighboring Hb. Since the effect is manifested in τ_c, only hydrodynamic phenomena could so depend on concentration. Again, we cannot pursue such complexities.

The exchange terms k_t for H_2O and HDO are not accurately determined at 20 MHz, and accuracy becomes progressively worse as the frequency is lowered, since the rapidly increasing R_{1a} dominates. Nevertheless, the WS experiments give a unique measure of k_s (k_t), and we can make the following statements: (a) k_t is the same for H_2O and HDO at 20 MHz, for any concentration. (b) the concentration dependence of k_t is probably the same as R_2, although some wayward data points make this less certain. (c) k_t probably has a small frequency dependence; this is quite uncertain, due to inaccuracies at 10 and 5 MHz. (d) k_t is like a negative nuclear Overhauser effect (NOE). When eq 9 now is applied to the water–protein proton interaction, this means the linear τ_c term dominates. The sign is unambiguous, as direct examination of WS data such as Figure 4 shows. This is a most significant result, for it implies that a protein and water spin must stay in close proximity long enough for a flip-flop transition to occur. This transition is due to the ($I_+S_- + I_-S_+$) interaction (Solomon, 1955) and superficially seems independent of field strength, since for like spins, the first term in k_t (eq 9) does not contain the Larmor frequency. Classically, the flip-flop term arises because one nucleus feels the time-varying magnetic field of a precessing neighboring nucleus, so for like nuclei, they are always "on resonance", no matter what the field. But the two nuclei must stay in close proximity long enough to experience at least a few Larmor precessions, which puts a stringent lower limit on the lifetime of a water in the first hydration layer. At 20 MHz, the Larmor period is 8×10^{-9} s, so the mean hydration lifetime should be a few times 10^{-8} s to enable the k_t process. We still observe the (negative) spin transfer at 5 MHz, which mandates a lifetime of about 10^{-7} s.

These are very long lifetimes, so it is important to estimate how many such water molecules are needed to yield the measured k_t. The flip-flop portion of the dipolar interaction is about one-third of the interaction responsible for T_2 [this is from the so-called three-halves effect for like nuclei (Abragam, 1961)]. The total T_2 is at most the rigid lattice value. This is highly orientation dependent, but for a water molecule in a hydrated crystal such as gypsum, the maximum splitting is about 10 G, due to the proton pair at a distance of 1.5, Å (Pake, 1948). Averaging over orientation, this would give a T_2 of about 15 μs ($R_2 = 6.7 \times 10^4$ s^{-1}), so the flip-flop rate is 2.2×10^4 s^{-1} for 1.5 Å. For an HDO adjacent to a protein spin, the distance is more likely the intergroup 2.5 Å, so finally we estimate the average rigid-lattice flip-flop rate of a protein–HDO proton pair as 1.4×10^3 s^{-1} Perhaps this should be reduced to a root mean square value, because of the random protein orientation, or perhaps increased by a factor of 2 or 3, since this interaction could well be with more than one protein spin. Nevertheless, it should be a good order of magnitude estimate. Since we measure $k_t = 0.1$ s^{-1} in a 3 mM Hb solution, then only one water molecule out of 1.4×10^4 need be attached to the protein for a time longer than a few Larmor periods. How much longer is irrelevant, so long as it is less than the reciprocal rigid-lattice value; i.e., we assume the off-rate is not the rate-limiting quantity for k_t.

To follow this through, one should finally estimate how many such sites need exist per protein molecule. The area of protein surface occupied by a water molecule has been estimated as 20 Å^2 (Rupley et al., 1983). Taking the Hb molecule as a sphere with a Stokes radius of 31 Å, there is room for 605 hydration water molecules, or 1210 water protons per protein. For 3 mM Hb, the water proton molarity is 94.6 M, or 3×10^4 water protons per Hb. Hence, only about two long-liver water sites per Hb are needed to account for the measured k_t. Tumbling should only effect the amplitude of the interaction, since the tumbling correlation time of 10^{-7} s is 10 times longer than our longest Larmor period. That is, random angle variation just modulates the strength of the Larmor field seen at the water site, not its frequency; hence, the root mean square value is used above.

If there were a larger number of sites with lifetimes longer than 10^{-8} s, we would see a much larger transfer rate, so we have an upper limit on the lifetime of the vast majority of the water molecules in the first hydration layer. Some hindered rotation of the hydration water might reduce the interaction and predict a somewhat larger number of sites, but it would still be orders of magnitude fewer than the 1200 proton sites on a sphere. Furthermore, the protein is not a smooth sphere but has many interstices, giving as many as 50% more sites (Chothia, 1984).

With so few exchange sites needed, one should seriously consider the possibility that atomic hydrogen exchange alone can account for all of the spin transfer. A fairly accessible exchangeable protein proton would exchange with a water proton via any of three mechanisms: acid-catalyzed exchange, base-catalyzed exchange, and neutral exchange. The exchanges observed in an NMR experiment are in the time range of milliseconds or less and so involve quite different hydrogens than are measured in tritium exchange work, but the class of exchange times of a few seconds or less comprises some 20% of all exchangeable protons (Benson et al., 1973).

If atomic exchange were indeed important, than the water T_2 would also be affected, that is, the exchange formulation of eq 2–4 would be valid for T_2 also. The intrinsic T_{2p} are multivalued, but all are much faster than T_{2a}. By use of an average T_{2p} of 1 ms, assuming T_{2a} can be neglected (the most conservative choice) and assuming fast exchange (i.e., more rapid than R_{2p}), the measured R_{2-} would be R_{2p} times the fraction of time a water proton is part of the protein spin system. For 4.7 mM Hb, we measure $R_{2-} = 5.0$ s^{-1}, and $R_{2p} = 1000$ s^{-1}; hence, the fraction is 0.005. Water molarity is 86 M, or 18 300 water protons per Hb, so 92 sites per Hb would need to have exchange lifetimes of 1 ms or less. Out of 4664 Hb protons, 928 are exchangeable, and half of these exchange too fast to detect by tritium exchange, i.e., a few seconds or less (Benson et al., 1973). How many are a millisecond or less is unknown, but it could be a significant number. The base-catalyzed exchange rate of an exposed side-chain amide at pH 7 is the diffusion-limited 10^{10} [OH] = 10^3 s^{-1} (Englander & Kallenbach, 1984), and in buffered solution it could be as fast as $10^{3.5}$ s^{-1} (Englander et al., 1972). The role of neutral exchange is difficult to judge. For the slow class of exchangable protons in BPTI, neutral exchange accounts for 93% of the total hydrogen exchange at the pD minimum of 4.5 (Hilton & Woodward, 1979; Gregory et al., 1983).

If the water T_2 is indeed due to hydrogen exchange, then its temperature dependence shows that it is fast exchange on the NMR time scale. That is, if the measured R_2 was the off-rate, then this rate would surely increase with temperature, whereas we observe the opposite. This is about the most definite statement we can make about this potential relaxation

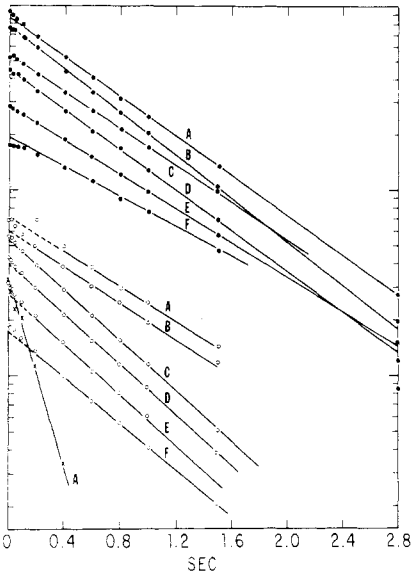

FIGURE 12: Magnetization recovery curves for water protons (top curves A–F) and aliphatic Hb protons (bottom curves A–F), at 200 MHz, 5 mM, and 25 °C, for various solvent mixtures. H_2O percentages are (A) 100%, (B) 90%, (C) 80%, (D) 70%, (E) 50%, and (F) ca. 1%. The fast protein component of (A), shown by (×), is obtained by subtracting dashed extrapolation from the data. Amplitudes are all relative in order to distinguish data.

mechanism, but it is clear that hydrogen exchange could well be one of several simultaneously occurring processes contributing to T_2 and k_t. To further complicate interpretation, there are large isotope effects on proton exchange (Englander et al., 1972).

Hydrogen exchange would also have important implications for the T_1 of water, since T_1 approaches T_2 at low frequencies. But it could not explain the major part of the dispersion, since a large dispersion very similar to that of water has been recently observed (Bryant & Jarvis, 1984) by using the protons of dimethyl sulfoxide in D_2O.

Finally, we should emphasize the hidden frequency dependence of the "frequency-independent" flip-flip spin-transfer mechanism. As pointed out above, the water and protein spins must stay in close contact for at least several Larmor periods for this interaction to actuate. When T_1 is measured over a wide frequency range, this can encompass a wide range of hydration lifetimes. At 5 MHz, a lifetime of at least 10^{-7} s is needed, and it is doubtful that many such hydration sites exits. But for the 200-MHz results discussed below, 2×10^{-9} s would be effective, and many more water protons might partake of spin transfer. This appears to be the case.

A limited amount of high-frequency data was taken. At 100 MHz, R_{1p} is still several times larger than R_{1a}, and qualitatively, an INV experiment (the only type done with the FT spectrometers) gives results similar to those at low frequencies, single exponential T_1 for aliphatic and water protons. At 200 MHz, T_1 becomes multiexponential, and the magnitude of k_s does seem much larger than at 20 MHz, consistent with the above remarks on the flip-flop mechanism. Figure 12 shows how the water and aliphatic protons relax after a nonselective 180° pulse, for a range of solvent composition from 100% H_2O (A) to nearly 100% D_2O (F). The amplitude scale is only relative, in order to separate the data.

Qualitatively, we expect that, at high frequencies, the local T_1 of methyl protons will be much faster than those of other protein and water protons, and thus, methyl protons act as relaxation sinks for all protons, assuming that spin diffusion to them is rapid. Since methyl groups are widespread and spin diffusion was fast enough at 20 MHz, protein spin mixing should be quite good at 200 MHz. In D_2O, the net R_{1p} would then be the methyl R_1 reduced by the ratio of methyl to total proton number. It is interesting that precisely this effect is seen at the opposite extreme condition, solid protein at low temperatures (Andrew et al., 1982). There all τ_c values except that of methyl rotation are too long to contribute to T_1 (eq 7). For our D_2O sample at 200 MHz, the aliphatic R_{1p} is 1.4 s^{-1} and the methyl fraction is 0.304, so the methyl relaxation rate is 4.6 s^{-1}, in good agreement with the value in column 9 of Table II, where $\tau_r = 10^{-10}$ is merely assumed.

As the solvent becomes more protonated, water protons are added to the relaxation pool, and since the intrinsic R_{1a} must be very slow at 200 MHz, the methyl protons are the relaxation sink for the solvent also. If spin exchange at the protein–water interface were very rapid, all protons in the solution would have the same T_1, now the methyl T_1 reduced by a much larger factor. The results of Figure 12 are not so simple but show many of the expected features of two-phase exchange, particularly the protein relaxation.

The protein T_1 in D_2O is entirely R_{1p}, since k_s is negligible; it is 1.4 s^{-1}. Then the value in H_2O should be 20% smaller, since there are 20% more non-methyl protons, i.e., 1.1 s^{-1}. The fast protein component in H_2O [the (×)'s of curve A in Figure 12] gives $\phi_{1+} = 5.9$; by use of eq 6a and $N_P/N_A = 0.275$ for 5.0 mM Hb, $k_s = 3.6$ and $k_t = 1.0$ s^{-1}. In D_2O, the k_t value for HDO protons should only be slightly reduced, and when R_{1a} and k_s are negligible, ϕ_{1-} is exactly k_t, in excellent agreement with the measured value of 0.9 s^{-1}, curve F for water protons. However, there remain the following discordant facts: A negative fast water component M_{A+} is observed for the D_2O sample as it should be but is much smaller than eq 4c predicts. The protein M_{P-} in curve F should be negligible, and is, but there is a small initial nonexponentiality lasting about 100 ms, present in all samples B–F. We would guess this is some initial mixing of protein spins, although it is considerably longer than at 20 MHz (Figure 5). The slow components in H_2O, both for water and for protein spins, are about a factor of 2 faster than calculated and are not quite equal, as they should be for strict two-phase exchange, i.e., all spins asymptotically relaxing to equilibrium as a unit. Despite this, the preliminary results for determination of the spin-exchange rates over a wide frequency range *above* the dispersion frequency show promise as a novel method to scan the hydration water lifetimes.

Summary and Conclusions

We have presented a very detailed study of NMR relaxation of the hemoglobin–water proton spin system. Although limited to one protein, all of the interpretations and conclusions should apply to other globular proteins as well. We have carefully verified the validity of the two-phase spin-exchange formalism as applied to T_1 behavior, enabling the intrinsic protein and water spin–lattice relaxation times to be obtained separately, as well as the spin-transfer rates between the two systems. Separate T_2's have also been extracted, and all quantities were measured at various concentrations, at two temperatures, at several frequencies, and in H_2O and D_2O, to give a rather complete overview of dipolar relaxation. Despite this, when attempting to interpret the molecular mechanisms responsible for relaxation, many of the same difficulties found by others persist here. Protein proton relaxation conforms reasonably to a simple model of dipolar relaxation of a rigid assembly of protons, in the lower frequency range, but no simple model of water dynamics in the hydration region can explain all of the results. Perhaps the most provocative result is the measured spin-transfer rate. It is inaccurate due to its smallness,

but this very smallness shows in a unique way that out of a geometrically possible 1200 water proton hydration sites, there can be no more than about five with water liftimes longer than 10^{-8} s.

REFERENCES

Abragam, A. (1961) *The Principles of Nuclear Magnetism*, Chapter 8, Clarendon Press, Oxford.

Andrew, E. R., Bone, D. N., Bryant, D. J., Cashell, E. M., Gaspar, R., Jr., & Meng, Q. A. (1982) *Pure Appl. Chem. 54*, 585–594.

Benson, E. S., Fanelli, M. R. R., Giacometti, G. M.; Rosenberg, A., & Antonini, E. (1973) *Biochemistry 12*, 2699–2706.

Bernhardt, J., & Pauly, H. (1975) *J. Phys. Chem. 79*, 584–590.

Bryant, R. G., & Jarvis, M. (1984) *J. Phys. Chem. 88*, 1323–1324.

Carr, H. Y., & Purcell, E. M. (1954) *Phys. Rev. 94*, 630.

Chothia, C. (1984) *Annu. Rev. Biochem. 53*, 537–572.

de Witt, J. L., Hemminga, M. A., & Schaafsma, T. J. (1978) *J. Magn. Reson. 31*, 97–107.

Eisenstadt, M. (1980a) *J. Magn. Reson. 38*, 507–527.

Eisenstadt, M. (1980b) *J. Magn. Reson. 39*, 275–290.

Eisenstadt, M. (1980c) *J. Magn. Reson. 39*, 263–274.

Eisenstadt, M. (1981) *Biophys. J. 33*, 469–474.

Eisenstadt, M., & Fabry, M. E. (1978) *J. Magn. Reson. 29*, 591–597.

Englander, S. W., & Kallenbach, N. R. (1984) *Q. Rev. Biophys. 16*, 521–655.

Englander, S. W., Downer, N. W., & Teitelbaum, H. (1972) *Annu. Rev. Biochem. 41*, 903–924.

Fabry, M. E., & Eisenstadt, M. (1978) *J. Membr. Biol. 42*, 375–398.

Freeman, R., & Hill, H. D. W. (1971) *J. Chem. Phys. 54*, 301–313.

Gregory, R. B., Crabo, L., Percy, A. J., & Rosenberg, A. (1983) *Biochemistry 22*, 910–917.

Grosch, L., & Noack, F. (1976) *Biochim. Biophys. Acta 453*, 218–232.

Hallenga, K., & Koenig, S. H. (1976) *Biochemistry 15*, 4255–4263.

Hasted, J. B. (1973) *Aqueous Dielectrics*, Chapter 8, Chapman and Hall, London.

Hilton, B. D., & Woodward, C. K. (1979) *Biochemistry 18*, 5834–5841.

Hindman, J. C., Svirmickas, A., & Wood, M. (1973) *J. Chem. Phys. 59*, 1517–1522.

Jardetzky, O., Ribeiro, A. A., & King, R. (1980) *Biochem. Biophys. Res. Commun. 92*, 883–888.

Kalk, A., & Berendsen, H. J. C. (1976) *J. Magn. Reson. 24*, 343–366.

Keller, K. H., Canales, E. R., & Yum, S. I. (1971) *J. Phys. Chem. 75*, 379–387.

Kimmich, R., & Noack, F. (1970) *Z. Naturforsch. A 25*, 1680–1684.

Koenig, S. H. (1980) *ACS Symp. Ser. No. 127*, 157–176.

Koenig, S. H., & Schillinger, W. E. (1969) *J. Biol. Chem. 244*, 3283–3289.

Koenig, S. H., Bryant, R. G., Hallenga, K., & Jacob, G. S. (1978) *Biochemistry 17*, 4348–4358.

Kuntz, I. D., Jr., & Kauzmann, W. (1974) *Adv. Protein Chem. 28*, 239–345.

Lankhorst, D., Schriever, J., & Leyte, J. C. (1982) *Ber. Bunsenges. Phys. Chem. 86*, 215–221.

MacDonald, C. C., & Phillips, W. D. (1969) *J. Am. Chem. Soc. 91*, 1513.

Meiboom, S., & Gill, D. (1958) *Rev. Sci. Instrum. 29*, 688.

Merck Index (1968) 8th ed., p 521, Merck & Co., Rahway, NJ.

Nemethy, G., & Scheraga, H. A. (1964) *J. Chem. Phys. 41*, 680–689.

Packer, K. J. (1977) *Philos. Trans. R. Soc. London, Ser. B 278*, 59–87.

Pake, G. E. (1948) *J. Chem. Phys. 16*, 327.

Rupley, J. A., Gratton, E., & Careri, G. (1983) *Trends Biochem. Sci. (Pers. Ed.) 8*, 18–22.

Saunders, M. A., Wishnia, A., & Kirkwood, J. (1957) *J. Am. Chem. Soc. 79*, 3289–3290.

Shirley, W. M., & Bryant, R. G. (1982) *J. Am. Chem. Soc. 104*, 2910–2918.

Solomon, I. (1955) *Phys. Rev. 99*, 559–565.

Sykes, B. D., Hull, W. E., & Snyder, G. H. (1978) *Biophys. J. 21*, 137–146.

Tanford, C. E. (1961) *Physical Chemistry of Macromolecules*, p 359, Wiley, New York.

Thompson, B. C., Waterman, M. R., & Cottam, G. L. (1975) *Arch. Biochem. Biophys. 166*, 193–200.

Vold, R. L., Vold, R. R., & Simon, H. E. (1973) *J. Magn. Reson. 11*, 283.

Wagner, G., & Wuthrich, K. (1982) *J. Mol. Biol. 155*, 347–366.

Winter, F., & Kimmich, R. (1982) *Mol. Phys. 45*, 33–49.

Zipp, A., James, T. L., Kuntz, I. D., & Shohet, S. B. (1976) *Biochim. Biophys. Acta 428*, 291–303.